

ADSORPTION AND DECOMPOSITION OF AMMONIA ON A W(110) SURFACE: PHOTOEMISSION FINGERPRINTING AND INTERPRETATION OF THE CORE LEVEL BINDING ENERGIES USING THE EQUIVALENT CORE APPROXIMATION

M. GRUNZE

Fritz-Haber-Institut der Max-Planck-Gesellschaft, Faradayweg 4–6, D-1000 Berlin 33, Fed. Rep. of Germany

C.R. BRUNDLE

IBM Research Laboratory, San Jose, California 95193, USA

and D. TOMÁNEK

Institut für Theoretische Physik der Freien Universität Berlin, D-1000 Berlin 33, Fed. Rep. of Germany

Received 10 March 1982; accepted for publication 29 April 1982

We report the first XPS data for ammonia adsorption, condensation and decomposition on a W(110) surface. Monolayer, “second layer” and multilayer NH_3 as well as NH_2 , NH and N^* species can be characterized by a specific N(1s) electron binding energy. We discuss the observed binding energies within a thermodynamic framework, using the “equivalent core approximation”. This model has been previously successfully applied to core level binding energies of gaseous molecules and solids. The agreement between calculated and experimental N(1s) binding energies for some species is excellent, and we conclude that for the considered adsorbates the variation of the N(1s) binding energies is primarily determined by the ground state properties rather than by different relaxation energies in the final state. We also briefly discuss the activity of the W(110) face towards NH_3 decomposition and also present some data for NH_3 dissociation on an oxygen preadsorbed surface.

1. Introduction

Adsorption and decomposition of ammonia on various metal surfaces has been studied in order to obtain a better understanding of the reaction mechanism of ammonia synthesis [1]. Surface spectroscopies have been applied to identify the nature of the reaction intermediates, and direct evidence has been obtained that, under low pressure conditions on metal surfaces, ammonia decomposes via amine and imine surface complexes to chemisorbed atomic nitrogen and hydrogen.

We present here the first XPS study of ammonia adsorption and decomposi-

tion on a tungsten single crystal surface. With adsorption at 80 K, the formation of monolayer, "second layer" and multilayer of NH_3 can be distinguished by XPS. The intermediates in the NH_3 dissociation reaction ($\text{NH}_{2,\text{ad}}$, NH_{ad} and N_{ad}) can all be isolated and fingerprinted by XPS. There is also a slight distinction between N_{ad} and a surface nitride species.

The experimentally determined differences in N(1s) electron binding energy between the various adsorbates can be explained by a thermodynamic model making use of the "equivalent core approximation" for the core-excited state. We apply here a simple extension of the model used by Jolly [2] to obtain core level binding energies in gas phase molecules and by Johansson et al. to estimate electron binding energies for solids [3].

Our studies of NH_3 interaction with an oxygen predosed surface confirms the observation made on other metals [4], i.e. that chemisorbed oxygen stabilizes the molecular integrity of the adsorbed NH_3 molecule against dissociation and increases its heat of adsorption.

2. Experimental

The experiments on the W(110) surface were carried out in a combined XPS/UPS/LEED/SIMS spectrometer (Vacuum Generators) [5]. The angle between the X-ray source (Mg $\text{K}\alpha$) and analyser is 115° and spectra reproduced here were collected at an angle of 40° with respect to the surface normal. The oriented W(110) crystal was mounted on a tantalum support and heated by electron bombardment from a tungsten filament placed behind the crystal. Cooling to 80 K was achieved by pumping liquid nitrogen through the probe. Temperature measurements were obtained by a W/W-Re thermocouple spotwelded to the tantalum support. Due to experimental difficulties, temperature readings above 80 K are not considered to be more accurate than ± 20 K.

The tungsten crystal was cleaned by flashing in an oxygen ambient and in vacuum until the XPS bands of impurities were within the noise level of detection.

The procedures for taking the presented spectra on the Fe(110) surface have been described previously [6].

Coverages of NH_3 and its decomposition products were determined by comparison of the XPS W(4f)/N(1s) intensity ratio to the W(4f)/O(1s) intensity ratio found for the optimum $p(2 \times 1)$ O LEED pattern formed by exposure of the W(110) crystal to oxygen at 300 K [24]. The theoretical N(1s)/O(1s) cross section ratios of Scofield [7] were used. As has been shown by us [30], the accuracy of coverage determinations by comparison of XPS intensities critically depends on the electron take-off angle and the relative position of the adsorbate to the surface plane. The adsorbate N(1s) emission of N_2 , NH_3 , NH and N relative to the O(1s) band of a known coverage ($\pm 15\%$) has been followed as a function of electron take-off angle, and therefore the

error involved in estimating absolute coverages for these species is close to the error in oxygen coverage of $\pm 15\%$.

3. Adsorption at 80 K

In fig. 1, a sequence of N(1s) spectra from adsorbed molecular ammonia with increasing coverage is shown. Initial exposure leads to the appearance of a N(1s) band centered at 400.9 eV below E_F with a half-width of 1.6 eV (fig. 1a). The coverage corresponding to spectrum 1a is $\theta \sim 0.2$ or $\sim 2.8 \times 10^{14}$ molecules cm^{-2} . With increasing coverage, the band shifts slightly to lower binding energies and increases in half-width ($E_B = 400.7$ eV, $\Delta = 2.05$ eV). The coverage for spectrum 1b is $\theta \sim 0.45$ (6.3×10^{14} molecules cm^{-2}). The shift and increase in half-width with coverage resembles the results of Fisher for NH_3 on Pt(111), who interpreted the change in terms of monolayer and "second layer" adsorption [8].

The equilibrium vapor pressure of NH_3 at 81.5 K is 10^{-10} Torr [9] and consequently, condensation is possible under our conditions for $p_{\text{NH}_3} > 10^{-10}$ Torr. Spectrum 1c is representative for a condensed ammonia layer of $\sim 24 \text{ \AA}$

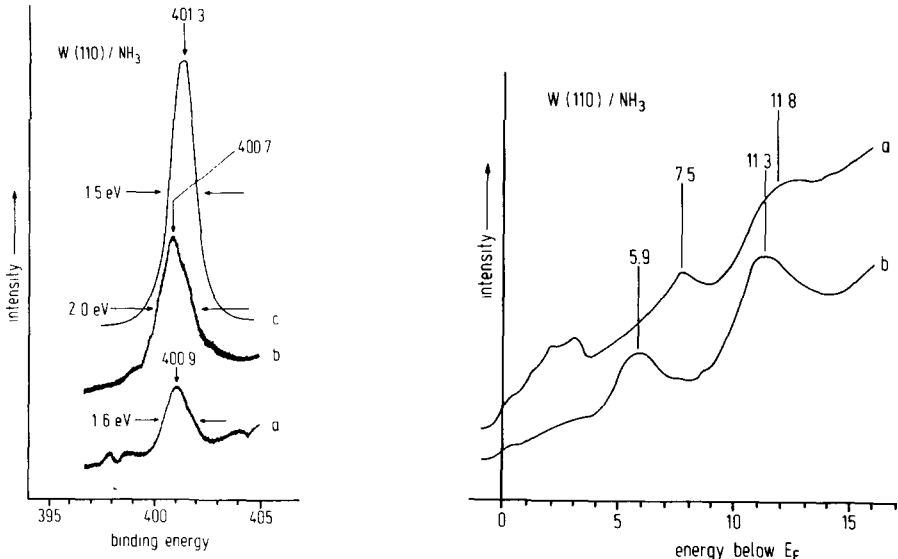


Fig. 1. Mg K α excited N(1s) core level spectra of molecular ammonia adsorbed at 80 K: (a) $\theta \sim 0.2$ ($\sim 2.8 \times 10^{14}$ molecules cm^{-2}); (b) "second layer" adsorption ($\theta \sim 0.45$); (c) condensed NH_3 (~ 6 layers) ($\times 2/3$).

Fig. 2. He II photoelectron spectra for NH_3 adsorption at 80 K: (a) $\theta \sim 0.2$; (b) beginning NH_3 multilayer formation.

thickness, as estimated from the attenuation of the W core level emission. The XPS band for condensed ammonia decreased in half-width ($\Delta = 1.4$ eV) and shifted to a higher binding energy of 401.3 eV.

We have also recorded He II UPS data for NH_3 adsorption at 80 K (fig. 2). In the multilayer adsorption regime, the $3a_1$ and $1e$ orbitals of molecular NH_3 are at 5.9 and 11.3 eV, respectively, with a separation very close to the gas phase value. For initial adsorptions, a strong "bonding shift" of the $3a_1$ orbital is observed, the $3a_1$ and $1e$ values being 7.5 and 11.8 eV, respectively. The shift of the non-interacting $1e$ orbital in going from first layer chemisorbed to multilayer adsorption of 0.5 eV is comparable to the observed N(1s) shift of 0.4 eV (see fig. 1).

4. Decomposition of NH_3

In order to identify the stable intermediates in the decomposition reaction, we heated the ammonia-covered surface stepwise to higher temperatures. The subsequent spectra were recorded during cooling to 80 K again, therefore readsorption of molecular ammonia from the background ($p \leq 2 \times 10^{-10}$ Torr) cannot be excluded, but should contribute only marginally to the intensity of the 400.8 eV band.

Heating an ammonia-dosed surface (fig. 3a) to ~ 170 K results in the appearance of a low binding energy shoulder on the molecular NH_3 band at 398.8 eV below E_F (fig. 3b). With increasing flash temperature (figs. 3c and 3d) this shoulder shifts to lower E_B values, and two bands centered at 397.8 and 400.8 eV below E_F become resolvable. As will be discussed later, we identify the 398.8 eV band as emission from NH_2 surface complexes. The shift of this shoulder to 397.8 eV then indicates further dissociation of the NH_2 species to NH surface molecules.

Spectrum 3f obtained after heating the predosed surface to room temperature is identical to a spectrum recorded after adsorption at 300 K and shows only one band at 397.8 eV, which we ascribe to NH surface fragments. After flashing the crystal to $T > 600$ K, this band shifts further to 397.3 eV, indicating the fission of the last N-H bond with atomic nitrogen remaining on the surface.

As pointed out, the spectra in fig. 3 are partly obscured by readsorption of ammonia during the time necessary to collect the spectra. In a separate experiment, we determined the percentage of decomposition by dosing at 80 K and directly heating to 300 K. Of the initially adsorbed ammonia ($\theta \approx 0.45$) 28% decomposes into NH species, while the rest desorbs up to 300 K as NH_3 . The subsequent transformation of NH to N is quantitative.

Exposing the W(110) surface to NH_3 at temperatures above the transition temperature from NH to N leads to the formation of "surface nitrides" and eventually, of course, to the formation of bulk nitride phases. The formation of

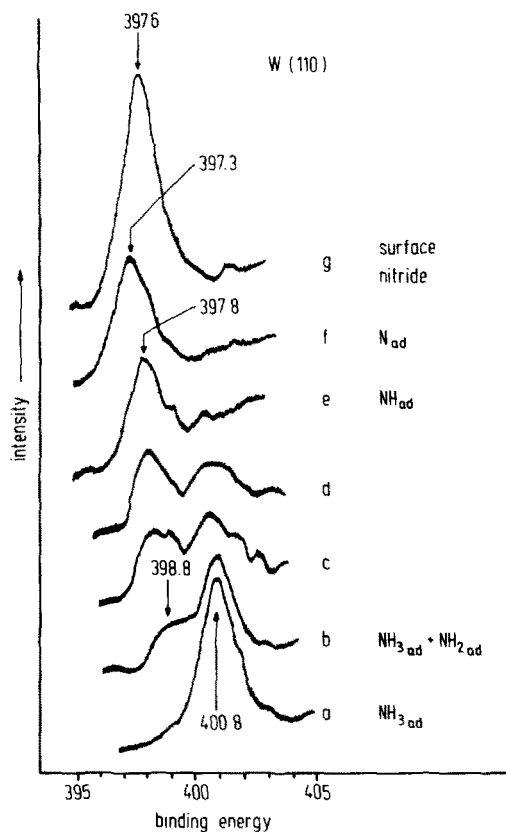


Fig. 3. Decomposition of NH₃ on a W(110) surface by heating the predosed surface to the following temperatures: (a) molecular NH₃ at 80 K; (b) ~170 K; (c) ~210 K; (d) ~260 K; (e) 300 K; (f) ~600 K; (g) "surface nitride" formed by exposing the substrate NH₃ at ~600 K.

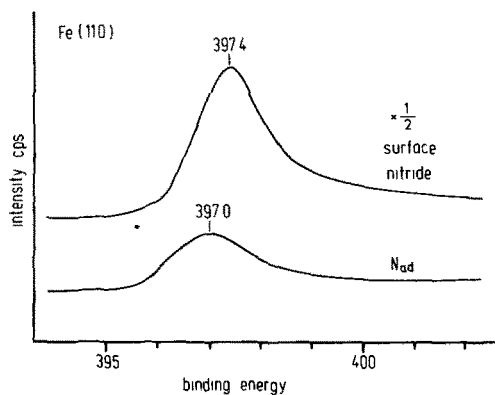


Fig. 4. N(1s) spectra of submonolayer adsorbed nitrogen and a "surface nitride" on a Fe(110) surface.

such a three-dimensional surface compound is reflected in the XPS data by a shift of the N1s band to a slightly higher binding energy of 397.6 eV (fig. 3g). This N(1s) binding energy shift to higher binding energies with the incorporation of nitrogen into the selvedge is also observed on a Fe(110) surface. In fig. 4, we show the N(1s) spectra of atomic nitrogen adsorbed on a Fe(110) surface and the spectrum corresponding to a "surface nitride" as defined by LEED experiments [10]. Again, a slight shift to higher E_B values is apparent.

5. Decomposition of NH₃ on an oxygen predosed W(110) surface

Recent results on ammonia adsorption on a Ni(111) surface [4] suggested that coadsorbed oxygen leads to azimuthal ordering of the NH₃ molecules and increases the adsorption energy of molecular NH₃. On W(110), small amounts of coadsorbed oxygen also have a pronounced effect on the surface reactivity. In fig. 5, we compare the N(1s) spectra obtained after exposing a clean (fig. 5a) and an oxygen predosed W(110) surface ($\theta_O \sim 0.2$) (fig. 5b) to 360 L NH₃ at room temperature. As compared to fig. 5a, we note in fig. 5b that a smaller amount of species with a binding energy of 397.8 eV populates the surface and that, in addition, molecular ammonia is present in about equal amounts. We assume that the 397.8 eV band corresponds to NH species; this, however, need not to be true because coadsorbed oxygen could affect the N(1s) binding energy of adsorbed atomic nitrogen. While in fig. 1b clearly no emission corresponding to NH₂ species around 398.8 eV is seen, the "NH" band in fig. 1a tails to higher binding energies, possibly due to some residual NH₂ species. The O(1s) band in fig. 5c shows, after NH₃ exposure, a higher binding energy shoulder which could indicate the presence of OH groups formed through dissociation of NH₃, or could represent a H bond interaction between molecular ammonia and oxygen.

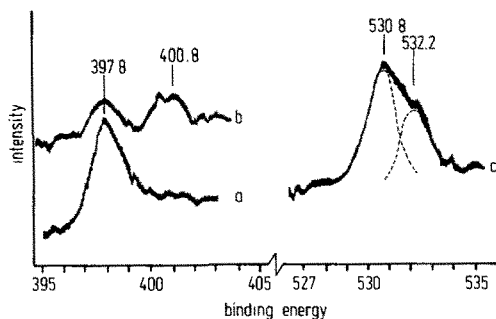


Fig. 5. Decomposition of NH₃ at room temperature on a clean (a) and oxygen precovered ($\theta \sim 0.2$) W(110) surface (b). The O(1s) spectrum (c) after NH₃ exposure shows a shoulder at 532.2 eV due to the formation of OH species.

6. Discussion of experimental data

We first want to compare our results for ammonia adsorption and decomposition to experimental data obtained on other transition metal surfaces. In table I we listed the so far reported N1s electron binding energies for the gaseous species and adsorbates on some transition metal surfaces. Results for molecular adsorbed N_2 have been included for the following discussions. For NH_3 on W(110) and Pt(111) [8], a small distinction can be made between ammonia adsorbed in submonolayer quantities and “second layer” NH_3 , which exhibits a somewhat smaller N1s binding energy. In the corresponding UPS spectra on Pt(111) [8] an obvious difference between these two states is evident from the increase in the $3a_1-1e$ separation going from monolayer to “second layer” adsorption. As first discussed by Grunze et al. [15] for monolayer adsorption on Fe(111), the gas phase separation between the $3a_1-1e$ orbital in NH_3 of 5.6 eV is reduced to 4.4 eV by the “bonding” shift of the $3a_1$ orbital to the substrate. On W(110), the $3a_1-1e$ separation is 4.3 eV for a fractional NH_3 coverage of $\sim \theta = 0.2$ (2.8×10^{14} molecules cm^{-2}). Increasing the coverage up to starting multilayer formation, the $3a_1$ and $1e$ orbital shift to 5.9 and 11.3 eV below E_F , respectively. Such a behavior was also found on Pt(111) for $\theta > 3.5 \times 10^{14}$ molecules cm^{-2} by Fisher [8]. Although a hexagonal close-packed NH_3 layer could accommodate 8.8×10^{14} molecules cm^{-2} [16], the increase of the $3a_1-1e$ separation to 5.4 eV at $\theta \sim 0.5$ indicates that the $3a_1$ orbital is not coupling directly to the substrate, i.e. NH_3 adsorbs in a “second layer”. That a distinct “second layer” NH_3 species forms upon exposure at $T \leq 100$ K (i.e. different from chemisorbed and condensed ammonia) was shown by us [26] using angular resolved XPS measurements. The observed small changes in the N1s core level binding energy with “second layer” formation will be discussed later on.

On the Fe(111), Fe(110) and Ni(110) surfaces the XPS identification of NH_2 and NH species was supported by complementary techniques such as UPS, isotopic exchange, thermal desorption and SIMS [1,10,14]. The corresponding binding energy differences on iron and nickel between NH_3 and NH and between NH and N are ~ 3 and ~ 0.4 eV, respectively. Very similar binding energy differences are found on W(110) with the proposed assignment of the N(1s) bands for NH and N surface species. The NH_2 surface molecule on Fe(111) was found to have a N(1s) binding energy around 398.5 eV, which is similar to the NH_2 binding energy observed on W(110). The analogy of our data to results obtained on other metal surfaces, therefore, suggests an assignment of the observed N(1s) bands to specific surface complexes (table I). It would, however, be desirable to support the identification of NH_2 and NH species on W(110) with other techniques.

Table 1
N(1s) electron binding energies (eV) for N-R (R = N, H) gaseous molecules and adsorbates on transition metal surfaces

Substrate	N ₂	NH ₃	NH ₂	NH	N	"Surface nitride"	Reference
Gas phase	409.9 ^{a)}	405.6 ^{a)}			411.0 ^{b)}		[11,12]
W(110)	399.1 400.5 ^{c)}	400.9 400.7 ^{d)} 401.3 ^{e)}	398.8	397.8	397.3	397.6	This work
Fe(110)				397.3	397.0	397.4	This work and ref. [6]
Fe(111)		400.0	~398.5	~397.0	396.6		[6]
Ni(110)	401.5 ^{c)}	400.9		398.4	398.0		[13,14]
Ni(100)	400.8 ^{c)}	400.2 399.8 ^{d)} 400.8 ^{e)}		~397.7	397.4		[26]
Pt(111)		399.9 399.3 ^{d)}					[8]

^{a)} Referenced to the vacuum level E^V

^{b)} Calculated via a Born-Haber cycle (see text).

^{c)} Refers to the "screened" final state at lower binding energies.

^{d)} "Second layer" NH₃.

^{e)} Condensed NH₃.

7. Calculation and thermodynamic interpretation of N(1s) binding energies

In the following, we present a thermodynamic model to account for the observed N(1s) electron binding energies of various species on W(110). The physical description is a simple extension of models based on the “equivalent core approximation”, which have been successfully used to obtain core level binding energies in gaseous molecules [2] and solids [3].

The measured binding energy of a core electron in an atom or molecule is equal to the energy difference between the initial neutral state and the final ionized state. In general, more than one discrete final state is possible, and therefore more than one binding energy is possible depending on the different possibilities for valence electrons to relax towards the core hole in an attempt to screen it. The relative probabilities of reaching these different final states depend on the overlap matrix between the initial state and final state. If the overlap to any given final state is greater than zero, then intensity will appear in the core level photoelectron spectrum at the binding energy corresponding to the transitions to this final state. For a molecule adsorbed on a metal, the lowest energy final state for a core transition process (and therefore the lowest observable binding energy peak, assuming it carries intensity) may correspond to a situation where an electron is effectively transferred from the metal Fermi level to an available valence level orbital of the adsorbed molecule lying below E_F . This is referred to as the “fully screened final state” and in it the adsorbate molecule is essentially neutral.

Within the equivalent core model, the final state of a core-ionized atom,

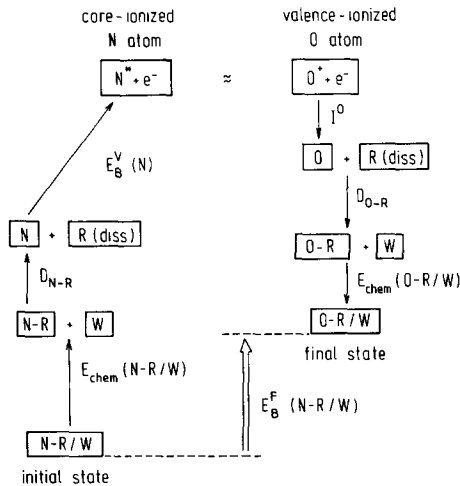


Fig. 6. Born-Haber cycle for the calculation of the N(1s) core level binding energy in a NR complex adsorbed on a tungsten surface. The N(1s) binding energy $E_B^F(N-R/W)$ refers to the fully screened N(1s) hole. The construction of the cycle is discussed in the text.

atomic number Z , has the same energy as that of a $Z + 1$ atom with its core level electrons all present, but its highest lying valence electron removed. Thus, N^* (1s hole) $\equiv O^+$ (2p hole). In the core of a *fully screened* N atom on a metal the final state would be N^{*-} (1s hole, plus screening electrons) $\equiv O$ (neutral). Therefore, within the equivalent core model and *assuming complete screening* the measured binding energy $N(1s)$ for a N–R species adsorbed in W(110) corresponds to the energy required to go from N–R/W(110) to O–R/W(110) as indicated in fig. 6. We can also construct an alternative route to this final state using a Born–Haber cycle, as shown in fig. 6. An analogous cycle could easily be set up for any other adsorption system.

Starting from the initial state, which is a N–R species adsorbed on a tungsten surface, we first have to overcome the chemisorption energy $E_{\text{chem}}(N-R/W)$ to desorb N–R. Next, N–R is dissociated into its constituent atoms, which requires the dissociation energy D_{N-R} . The total energy is further raised by the core ionization energy $E_B^V(N)$ of the nitrogen atom and we end up with a core ionized nitrogen atom N and an electron at the vacuum level. In the equivalent core approximation this nitrogen atom with a core hole is then equivalent to a valence ionized oxygen atom O^+ [2].

To get to the final situation, O–R/W, O^+ is required to release its ionization energy, I^0 , to combine with the R fragment atomic constituents and finally chemisorb to the W surface as indicated in the right-hand side of fig. 6.

From this cycle, the binding energy of a nitrogen core electron in a chemisorbed N–R species can be calculated as

$$E_B^F(N-R, W) = E_{\text{chem}}(N-R/W) + D_{N-R} + E_B^V(N) - I^0 - D_{O-R} - E_{\text{chem}}(O-R/W). \quad (1)$$

Note that the Born–Haber cycle gives the binding energy with reference to E_F and, therefore, is directly applicable to experiment.

In the case of a not completely screened $N(1s)$ hole final state, some modifications must be made only on the right-hand side of the Born–Haber cycle in fig. 6, since the equivalent core model replacement is no longer a neutral O in O–R/W but rather a partly positively charged O. Therefore, the whole ionization energy I^0 , will not be released, but only a fraction characterized by a screening parameter α ($0 \leq \alpha \leq 1$). The energies for association of the partially charged O atom with the R fragments and for the adsorption of the complex on the surface will change, and are generally expected to be higher than in the fully screened case.

Next, a few remarks concerning the screening probability of the adsorbate core hole in the final state. The screening parameter α , describing the substrate-to-adsorbate (and/or adsorbate-to-adsorbate) charge transfer, has to be estimated from case to case. Note, however, that within the simple model presented here, we do not distinguish between intra-molecular and inter-molecular screening and that the intra-atomic relaxation energy is included in the

$E_B^V(N)$ term. We expect a large value of α , if one of the final state molecular orbitals, unfilled in the initial state and mainly located in the adsorbate, overlaps with occupied substrate orbitals and lies near the Fermi energy of the substrate. Then it can be pulled below E_F and filled in the final state, due to the change in electrostatic potential upon photoemission. As the chemisorption energy generally increases with increasing overlap between the molecular and the substrate orbitals, we intuitively expect an improved screening going from a physisorbed to a chemisorbed state, provided a suitable screening orbital is available.

It is instructive to compare the core level binding energy of a chemisorbed species with that of a gaseous molecule. Apart from the work function of the substrate, two main contributions will determine the difference between their core level binding energies [17]. The first, the chemical shift, accounts for the change in the electrostatic potential at the nucleus upon adsorption. In eq. (1) this shift, which depends on the adsorption geometry and includes a possible charge transfer between adsorbate and substrate, is implicitly included in the chemisorption energy E_{chem} .

The second contribution is the relaxation shift, which accounts for the change in the intra-molecular and extra-molecular screening upon chemisorption. Energies connected with such relaxation processes are included mainly in term I^0 in eq. (1), although the other energy terms on the right-hand side of the cycle are affected as well through their dependence on the final state screening.

The use of eq. (1) to calculate the core level binding energy of an adsorbed species for the case of complete final state screening is straightforward, as the molecular dissociation energies D and the free-atom core excitation energy E_B^V can be taken directly from data tabulated for gaseous molecules. In addition, however, the knowledge of chemisorption energies is required. Clearly, as no atomic rearrangement takes place during the XPS process (Franck–Condon principle), the final state chemisorption energy has to be evaluated for the initial state geometry. In the systems considered, however, this quantity is believed not to depend sensitively on small changes in the geometry and hence is approximated by the corresponding ground state value.

In the case of an incomplete final state screening, the dissociation energies of partially charged molecules can be obtained from a gas-phase Born–Haber cycle by using tabulated bond and ionization energies. The chemisorption energy of a partially charged species can be estimated from the chemisorption energy of neutral adsorbates and from the interaction of a point charge with a jellium surface [18].

From the above discussion we conclude, that the presented Born–Haber cycle contains the complete information, though not a detailed insight, of the physics involved in the photoemission process. The decomposition of the core level binding energy into a sum of thermodynamic quantities helps moreover to provide quantitative predictions. In the following, we apply the Born–Haber cycle to predict N1s binding energies for nitrogen-containing species on a W(110) surface.

Table 2

Compilation of thermodynamic data used in the Born–Haber cycle and a comparison between predicted and observed N1s binding energies for different adsorbates; the upper part of the table corresponds to a completely screened final state ($\alpha=1$); in the lower part reduced screening

α	Adsorbate	$E_{\text{chem}}(\text{N-R/W})$ (1)	$D_{\text{N-R}}$ (2)	$\Sigma(1)+(2)$	$-I^0$ (3)
1	N ₂	0.5	9.8 ^{e)}	10.3	-13.6 ^{e)}
	NH ₃ (cond.)	0.3 ^{g)}	12.1 ^{e)}	12.4	-13.6 ^{e)}
	NH ₃ ($\theta \sim 0.45$)	0.4	12.1 ^{e)}	12.5	-13.6 ^{e)}
	NH ₃ ($\theta \sim 0.2$)	0.5 ^{b)}	12.1 ^{e)}	12.6	-13.6 ^{e)}
	NH ₂	2.6 ^{b)}	7.3 ^{e)}	9.9	-13.6 ^{e)}
	NH	3.8 ^{b)}	3.3 ³⁾	7.1	-13.6 ^{e)}
	N	6.4 ^{c)}	-	6.4	-13.6 ^{e)}
	Surface nitride	~ 5.4 ^{f)}	-	~ 5.4	-13.6 ^{e)}
0.5	NH ₂	2.6 ^{b)}	7.3 ^{e)}	9.9	-6.8

a) N(1s) level corresponding to the screened final states (see text).

b) Energies calculated from a Born–Haber cycle based on the Fe–NH_x bond energies from refs. [20,15] and corrected for the W–H bond strength taken from ref. [23].

c) Ref. [22].

d) Ref. [24].

e) Ref. [21].

f) Bond energies for high coverages as given in refs. [22,24].

g) Ref. [25].

In table 2 thermodynamic data used in the Born–Haber cycle are compiled together with the predicted and measured core level binding energies. The N(1s) binding energy of gaseous atomic nitrogen $E_B^V(\text{N})$ was calculated to be 411.0 eV via another Born–Haber cycle with a N₂^{*}–NO⁺ core exchange, using chemical reaction energies and the experimental value $E_B^V(\text{N}_2) = 409.9$ eV [11]. Such an approach has proven useful for calculating chemical shifts in simple gaseous N-containing molecules [2]. Note, that a possible error in the $E_B^V(\text{N})$ value would influence the following quantitative discussion of the experimental data.

In the calculated N(1s) binding energies, presented in table 2, complete screening has initially been assumed for all the adsorbates, except for the entry in the last line.

From comparison of the last two columns in table 2, we note a good agreement between the experimental and theoretical N(1s) binding energies for adsorbed N₂, NH₃ (low coverage θ) and N_{ad}. Whereas $\alpha = 1$ is expected for N_{ad} since it is located in the surface of the metal [30], a justification for the assumption $\alpha = 1$ is not directly evident for N₂ and NH₃. For chemisorbed N₂ a triplet structure has been observed. While the two main peaks at ~ 400 and ~ 406 eV have been ascribed to screened and unscreened final states, respec-

($\alpha=0.5$) is assumed for $\text{NH}_{2,\text{ad}}$; E_{chem} is the chemisorption bond energy between the adsorbate and the W(110) surface, and D is the dissociation energy of a molecule into atoms; all energies are in (eV)

$-D_{\text{O-R}}$ (4)	$-E_{\text{chem}}(\text{O-R/W})$ (5)	$\Sigma(3)+(4)+(5)$	$E_{\text{B}}^{\text{F}}(\text{theor.})$	$E_{\text{B}}^{\text{F}}(\text{exp.})$
$-6.5^{\text{e)}}$	$\gtrsim -0.4^{\text{h)}}$	$\gtrsim 20.5$	≤ 400.7	399.1 400.5 ^{a)}
$-8.5^{\text{e)l)}}$	$-0.48^{\text{g)}}$	-22.7	400.8	401.3
$-8.5^{\text{e)j)}}$	$\sim -0.6^{\text{j)}}$	-22.8	~ 400.9	400.7
$-8.5^{\text{e)l)}}$	$\sim -0.7^{\text{j)}}$	-22.9	~ 400.9	400.9 ^{a)}
$-9.6^{\text{e)}}$	$-0.7^{\text{i)}}$	-23.9	397.0	398.8
$-4.44^{\text{e)}}$	$\sim -4^{\text{k)}}$	~ -22	396.0	397.8
-	$-6.7^{\text{d)}}$	-20.3	397.1	397.3
-	$\sim -4.0^{\text{d)}}$	~ -17.6	~ 398.8	397.6
-10.1	-3 to -6	-20 to -23	398 to 401	398.8

^{h)} NO dissociates even at 100 K on W(110) [27]. We therefore assume $E_{\text{chem}} > E_{\text{diss}}$.

^{l)} Energies adapted from ref. [28].

^{j)} Estimates for the unstable OH_3 species, derived from H_2O data [28].

^{k)} Estimated from comparison with NH chemisorption energy.

^{l)} Ref. [32].

tively [19,29], further splitting of the “screened” peak into bands at 400.5 and 399.1 eV has not yet been understood. We find a good agreement between the calculated ($\alpha = 1$) and experimental binding energies for the peak at 400.5 eV, whereas the band at 399.1 eV cannot be explained by the thermodynamic data used in the Born–Haber cycle. For NH_3 it has been suggested [29] that a similar structure should exist, but the separation between screened and unscreened final states is barely resolvable experimentally.

Not shown in table 2 are data for the unscreened $\text{N}(1s)$ emission from N_2 , which is found experimentally at ~ 6 eV higher binding energy than the more intense screened state. Assuming $\alpha = 0$, corresponding to an absence of extra-atomic screening, the ionization energy I^0 would not appear in eq. (1), thereby raising the core level binding energy by 13.6 eV with respect to the unscreened case. On the other hand, this increase would be partially compensated by the higher dissociation and chemisorption energies of a charged species. With this argument, the position of the unscreened peak can qualitatively be understood. However, since the last-mentioned quantities are not accessible to experiment and hard to estimate, we did not include the unscreened peaks of N_2 in table 2.

From table 2, the assumption of complete final state screening for other species than N_{ad} , N_2 and NH_3 does not lead to such a good agreement between

theory and experiment. It should be noted, however, that even with $\alpha = 1$ the predicted binding energies generally follow the correct trend, i.e. they decrease with decreasing number of hydrogen atoms bound to the nitrogen atom and with decreasing nitrogen-to-substrate distance, which is reflected in an increasing chemisorption energy.

In addition, the values calculated for $\alpha = 1$ should always be smaller or equal to the experimental values, since experimentally $\alpha \leq 1$. In table 2 one can see that this is true (within an error of 0.2 eV) for all cases except the N_2 "screened doublet" discussed above and the surface nitride. Looking at the line of entries for the latter case we can see that there are three terms which are only approximately known. We assume, that this leads to a calculated value which is significantly too large (≥ 1.2 eV).

As compared to the $\alpha = 1$ case, for $\alpha < 1$ changes occur only in the Born-Haber terms of columns (3) to (5) of table 2. It has been mentioned earlier that, for the quantitative discussion, we need values of dissociation and chemisorption energies of partially charged species, which are often unstable or have not been studied experimentally. We, therefore, restrict our discussion to one example, the possible incomplete screening ($\alpha = 0.5$) of the final state of NH_2 , which is a partially ionized water molecule. In table 2, its dissociation energy has been calculated with the help of tabulated molecular bond and ionization energies [21]. The chemisorption energy of this charged adsorbate can be estimated from data for the uncharged N-R and O-R species and from the interaction energy of the adsorbate charge with a jellium substrate [18]. (Note that the electronic structure of an O-R⁺ species resembles that of an uncharged N-R rather than that of an O-R fragment.) The electrostatic energy has been calculated depending on the adsorbate-substrate distances which should be close to the molecular bond length [21], to range between 1 and 3 eV. This uncertainty gives rise to the large error bar for the chemisorption energy of the final state of NH_2 in the case of incomplete screening. Given the large error bar, the calculated value for $\alpha = 0.5$ now agrees with experiment.

In order to improve the agreement between theoretical and observed E_B^F values, reduced screening has to be postulated also for NH – this of course assumes, that the thermodynamic data used in the cycle are correct.

The question might arise as to why the calculated binding energies do not seem to depend more sensitively on the final state screening. The reason in our description is that for different screening situations, changes in quantities on the right-hand side of the Born-Haber cycle in fig. 6 partially compensate each other. However, the uncertainty in the thermodynamic data used in the cycle, in the case of reduced screening, does not allow a quantitative statement about the sensitivity of the predicted values on final-state screening. The above-mentioned compensation is nicely illustrated in the columns (3) to (5) of table 2, if NH_2 data for $\alpha = 0.5$ and $\alpha = 1$ are compared.

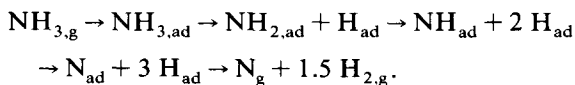
Additional information can be obtained from the photoemission data of

NH_3 as a function of coverage. Going from monolayer coverage to the condensed phase, changes occur in the chemical environment and consequently in the screening mechanism. For the multilayer situation, screening is reflected in the “solvent shift”, which can be observed in the binding energy of the N(1s) core level and the 1e valence level not directly involved in the bond formation. In the condensed phase, low extra-molecular screening is expected, which proceeds via the hydrogen bridge bonding. While the N(1s) binding energy for the plausible assumption of very low extra-molecular screening ($\alpha \ll 1$) might be expected to lie near the observed value, the predicted value for $\alpha = 1$ does not differ much from the experimental result. Hence, also in this case, comparison of predicted and experimental values is inconclusive with respect to establishing a value for α .

Summarizing the results presented in table 2, we observe a decrease in the N(1s) binding energy by going from $\text{NH}_{3,\text{ad}}$ via $\text{NH}_{2,\text{ad}}$ to N_{ad} . The parallel and more pronounced trend is observed in the total initial state energy, denoted $\Sigma(1) + (2)$ in the table. This trend is reduced, though not reversed, by the changes in the total final state energy, denoted $\Sigma(3) + (4) + (5)$. We thus conclude that, in the considered systems, the variation of the N(1s) binding energy is more determined by the ground state properties (“chemical shift”) rather than by relaxations in the final state [33].

8. Summary and conclusions

We have measured the N(1s) core electron binding energies on a W(110) surface for N_2 and NH_3 and its decomposition products. An identification of the chemical composition of the intermediates in the NH_3 dissociation reaction is possible by comparison to the data obtained on iron and nickel surfaces. Fragmentation of NH_3 occurs according to



On clean iron and nickel surfaces, molecular ammonia was found to be stable in equilibrium with its fragments at room temperature. On clean W(110), however, no spectroscopic evidence was found for molecularly adsorbed NH_3 after heating a NH_3 predosed surface to 300 K or exposing the clean surface at room temperature to NH_3 . This indicates a higher activity of the W(110) surface towards NH_3 dissociation as compared to the iron or nickel surfaces investigated. However, coadsorbed oxygen *increases* the molecular stability of adsorbed NH_3 through an energetic or kinetic effect as shown by our experiments on an oxygen predosed surface. This has also been demonstrated by Netzer and Madey on a Ni(111) surface using ESDIAD and thermal desorption techniques [4]. Accordingly, the valence-band photoemission results

for NH_3 adsorption would be expected to be critically dependent on the condition of the surface, a possible explanation for some contradictory results published for NH_3 adsorption on a Ni(110) surface [14,31].

In addition, we presented a thermodynamic description of the photoexcitation process in adsorbates and calculated the N(1s) binding energies in nitrogen-containing species on a W(110) surface using a Born–Haber cycle. Agreement (± 0.2 eV) between theory and experiment has been obtained for the fully screened final state of adsorbed N_2 (despite a discrepancy caused by a not understood triplet structure in the spectrum), NH_3 and atomic nitrogen. For other species, with the exceptions of the surface nitride, predicted values are less quantitatively correct, although they agree qualitatively, if full screening is assumed. In such species as $\text{NH}_{2,\text{ad}}$, NH_{ad} or condensed NH_3 quantitative agreement with experiment can be improved, if the final state screening is reduced. In this case, however, uncertainties in some quantities used in the Born–Haber cycle reduce the weight of the prediction.

It follows, from our discussion, that changes in the core level binding energies of adsorbed NH_3 and its decomposition products are mainly caused by a decrease in the total ground state energy, which is an initial state effect. We finally want to point out, that the presented description of the photoemission process might prove valuable to explain and predict core level binding energies also in other adsorption systems. It should be noted, however, that the dominant term in the Born–Haber cycle are the core level ionization values. Therefore, unless core level binding energies are measured very accurately, the reverse process of using measured binding energies to obtain chemisorption energies will not give values of high accuracy, even assuming that $\alpha = 1$ and all the other terms in the Born–Haber cycle are accurately known.

Acknowledgements

One of us (M. G.) would like to thank the IBM research laboratories for their hospitality and financial support during his stay in San Jose. This work was further supported by the Deutsche Forschungsgemeinschaft/ Sonderforschungsbereich 6. We also appreciated fruitful discussions with K.H. Benne-mann.

References

- [1] M. Grunze, in: *The Chemical Physics of Surfaces and Heterogeneous Catalysis*, Vol. 4, Eds. D.A. King and D.P. Woodruff (Elsevier, Amsterdam, in press).
- [2] For a review see, W.L. Jolly, in: *Electron Spectroscopy: Theory, Techniques and Applications*, Vol. 1, Eds. C.R. Brundle and A.O. Baker (Academic Press, 1978) 119 ff.
- [3] B. Johansson and N. Mårtensson, *Phys. Rev.* B21 (1980) 4427.
- [4] F.P. Netzer and T.E. Madey, *Phys. Rev. Letters* 47 (1981) 928.

- [5] C.R. Brundle, *IBM J. Res. Develop.* 22 (1978) 235.
- [6] M. Grunze, *Surface Sci.* 81 (1979) 603.
- [7] J.H. Scofield, *J. Electron Spectrosc.* 8 (1976) 129.
- [8] G.B. Fisher, *Chem. Phys. Letters* 79 (1981) 452.
- [9] C. Edelmann and H.G. Schneider, *Vakuumphysik und Technik (Akademische Verlagsgesellschaft, Leipzig, 1978)* p. 432.
- [10] M. Weiss, G. Ertl and F. Nitschke, *Appl. Surface Sci.* 2 (1979) 614.
- [11] U. Gelius, *J. Electron Spectrosc. Related Phenomena* 5 (1974) 985.
- [12] P. Finn, R.K. Pearson, J.M. Hollander and W.L. Jolly, *Inorg. Chem.* 10 (1971) 378.
- [13] M. Golze, M. Grunze, R.K. Driscoll and W. Hirsch, *Appl. Surface Sci.* 6 (1980) 464.
- [14] M. Grunze, M. Golze, R.K. Driscoll and P.A. Dowben, *J. Vacuum Sci. Technol.* 18 (1981) 611.
- [15] M. Grunze, F. Bozso, G. Ertl and M. Weiss, *Appl. Surface Sci.* 1 (1978) 241.
- [16] I. Olvsson and D.H. Templeton, *Acta, Cryst.* 12 (1959) 832.
- [17] N.D. Land and A.R. Williams, *Phys. Rev. B* 16 (1977) 2408.
- [18] N.D. Lang and W. Kohn, *Phys. Rev. B* 7 (1973) 3541.
- [19] P.S. Bagus, K. Hermann and M. Seel, *J. Vacuum Sci. Technol.* 18 (1981) 435.
- [20] G. Ertl, *Catalysis Rev. Sci. Eng.* 21 (1980) 201.
- [21] *CRC Handbook of Chemistry and Physics*, 55th ed. (The Chemical Rubber Company, Cleveland, Ohio, 1974).
- [22] P.W. Tamm and L.D. Schmidt, *Surface Sci.* 26 (1971) 286.
- [23] L.D. Schmidt, in: *Topics in Applied Physics*, Ed. R. Gomer, Vol. 4 (Springer, Berlin, 1975) p. 78.
- [24] T. Engel, H. Niehus and E. Bauer, *Surface Sci.* 52 (1975) 237.
- [25] D'Ans Lax, *Taschenbuch für Chemiker und Physiker*, Vol. 1 (Springer, Berlin, 1967).
- [26] C.R. Brundle and M. Grunze, in preparation.
- [27] R.I. Masel, E. Umbach, J.C. Fuggle and D. Menzel, *Surface Sci.* 79 (1979) 26.
- [28] C. Benndorf, C. Nöbl, M. Rösenberg and F. Thieme, *Surface Sci.* 111 (1981) 87.
- [29] P.S. Bagus and K. Hermann, in preparation.
- [30] C.R. Brundle, M. Grunze and D.A. King, in preparation.
- [31] K. Jacobi, E.S. Jensen, T.N. Rhodin and R.P. Merrill, *Surface Sci.* 108 (1981) 397.
- [32] B.W. William and R.F. Porter, *J. Chem. Phys.* 73 (1980) 5598.
- [33] This is not to be confused with the fact that the relaxation energy exceeds the chemical shift in magnitude.